



September 7. - 9.9.2009

Cheb, Czech Republic

# SIMULATION MODEL OF ELASTOMAGNETIC SENSORS

PROF. ING. DOBROSLAV KOVÁČ, CSc.

ING. MILAN PEŤKO

PROF. ING. IRENA KOVÁČOVÁ, CSc.

DOC. ING. VOJTECH ŠIMKO, CSc.

**Abstract:** An article says about the basic magnetic features of ferromagnetic material, which need to be taken to the consideration when designing model of elastomagnetic sensor. Mentioned is an intelligent calculator, which is used for calculation of change of sensor permeability in cubic grate in dependence of the lay of vectors of magnetostriction and external field. In the article, the sensor model in program PSPICE is described. Model in program PSPICE simulates a real hysteresis loop of sensor, his loses, his dependency from the frequency and the entry signal. Realized is by passive elements and controlled current sources the way it could simulates real entry signal and also the shape of the hysteresis loop. In the conclusion of the article, the hysteresis loop of real sensor of a torque is showed. The basic requirements for the sensor model were simplicity, accuracy, comprehensibility, open system and further utility for similar types of sensors.

**Key words:** simulation, controlled sources, hysteresis

## INTRODUCTION

One of the basic tasks of the measure technique is sensing, processing and evaluating of the measured magnitude. As because the solution of many electrical engineering problems by direct experimental examining of physical real system is sometimes quite difficult, it is more convenient to experiment by computer model. Every scientific and technical discipline has its specific issues when composing models. The example can be the modelling of the influence of features of ferromagnetic on the output parameters of elastomagnetic sensor force. It uses the knowledge of physic of magnetic elements, effect of magnetostriction, features of basic circuits.

## 1 ELASTOMAGNETIC EFFECT

Joule discovered effect of change of geometric dimension of ferromagnetic material under change of magnetization, called magnetostriction, in 1842. Magnetostriction effect is connected with thermodynamic opposite effect – elastic-magnetic, which was watched in 1865 by Villari. This effect functions when mechanic strain of ferromagnetic entity and changes its magnetic features, changes also the permeability of the material.

$$\left(\frac{\partial M}{\partial p}\right)_{H,\mathcal{G}} = \left(\frac{\partial w}{\partial H}\right)_{p,\mathcal{G}} \quad (1)$$

where:  $p$  is general pressure,  $M$  is magnetic polarization,  $w$  is relative deformation,  $H$  is intensity of magnetic field,  $\mathcal{G}$  is external temperature.

## 2 CHANGE OF PERMEABILITY

Own mechanism of influencing permeability by mechanic force consists in consequence of deformation on crystal grate of material. By its influence, a distance of the atoms in the grate changes an also the ration of this distance to the radius of atoms. Of this, the size of the energy of exchange forces depends, which cause agreed orientation of magnetic moments no-compensated spins and create the domains. A change of size of domain oriented in particular direction will be shown as change of magnetic polarization, or magnetization vector. After some modification we can reach the formula for the change of permeability:

$$\Delta\mu = \frac{2\lambda_{msstr}}{B_{sef}^2} \mu^2 \sigma \quad (2)$$

where:  $\lambda_{msstr}$  is middle value of coefficient of magnetostriction when saturation,  $B_{sef}$  is effective value of magnetic induction when saturation,  $\sigma$  is pressure.

### 3 MAGNETOSTRICTION

By influence of magnetic force on the entity, on which this force works, it deforms. Change of material shape describes a magnetostriction coefficient:

$$\lambda_m = \frac{\Delta l_m}{l_m} \quad (3)$$

Magnetostriction  $\lambda_m$  of ferromagnetic mono-crystals is characterized by anisotropy. Dependency  $\lambda_m$  has for several crystallographic directions different behaviour. Middle magnetostriction is calculated from magnetostriction in each directions of simple magnetization ( $\{100\}$ ,  $\{010\}$ ,  $\{001\}$ ). The most often case is to set the magnetostriction in direction of magnetising. For the magnetostriction in cubic grate in direction of magnetising is valid:

$$\lambda_v = \lambda_{100} + 3(\lambda_{111} - \lambda_{100})(\alpha_1^2\alpha_2^2 + \alpha_2^2\alpha_3^2 + \alpha_3^2\alpha_1^2) \quad (4)$$

#### 3.1 Intelligent calculator

Becker a Döring agreed to the conclusion that the magnetostriction of saturation can be described by directing cosines of vector of external magnetic field and of vector of magnetostriction with the axes of crystal material composition. From that reason an intelligent calculator was designed. In general practice, there are several types of crystal material composition. The most often and also the simplest is cubic crystal composition, e.g. iron or nickel.

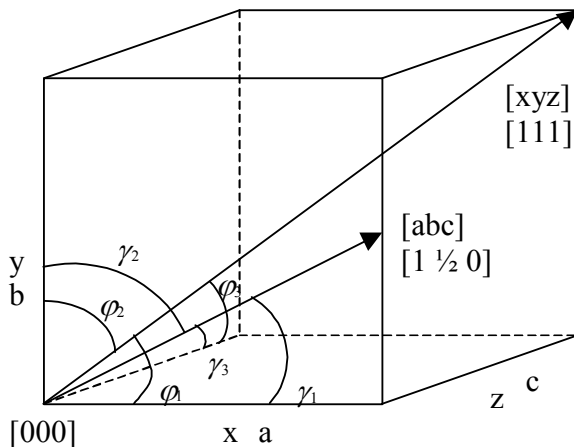


Fig. 1: Cubic crystal

For the cubic crystal on the Fig. 1. the magnetostriction saturation can be described as:

$$\lambda_s = \frac{3}{2}\lambda_{100}\left(\sum_{i=1}^3\alpha_i^2\beta_i^2 - \frac{1}{3}\right) + 3\lambda_{111}(\alpha_1\alpha_2\beta_1\beta_2 + \alpha_1\alpha_3\beta_1\beta_3 + \alpha_3\alpha_2\beta_3\beta_2) \quad (5)$$

where:  $\alpha_i = \cos \varphi_i$  a  $\beta_i = \cos \varphi_i$ .

Magnetostriction depends on direction of vector of magnetostriction  $[xyz]$ , direction of vector of external field  $[abc]$  and magnetostriction in directions  $\langle 100 \rangle$  and  $\langle 111 \rangle$ . Calculator shown on Fig. 2. is used for simple calculation of magnetostriction saturation for several directions of magnetostriction vector and vector of external field

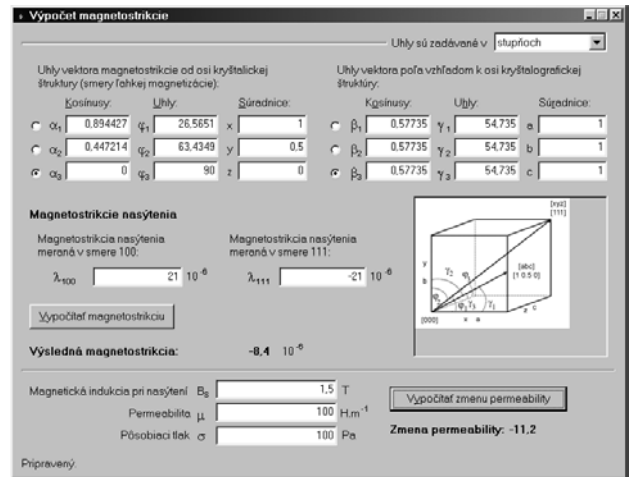


Fig. 2: Intelligent calculator

### 4 MODELLING OF HYSTERESIS LOOP

Using AC magnetic field the magnetic material reports a hysteresis, see Fig. 3.

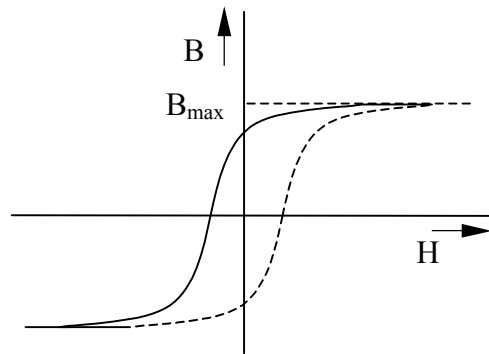


Fig. 3: Hysteresis loop

Hysteresis comes up due to errors (dislocation) of the material, late delivery of buds counter domains, what causes creation of heat loses in the material. The material heat loses are relative to the area of hysteresis loop. Hysteresis loop depends of used material and external field intensity. By effect of magnetic charging of magnetic material, it goes the change of permeability and the change of the hysteresis loops changes. In software PSIPCE, there are several models, the most famous one is called Jiles-Atherton model. When using Jiles-Atherton model, it is necessary to know the values of material

constants. Total sensitivity and characteristic of output value than depends on accurate assignment of these constants. Jiles-Atherton model is from the modelling point of view and simulation demanding on calculation and on accuracy of assigning material constants, which can be found only by experimenting. For his versatility and possibility to get modified is very spread and used for modelling of hysteresis loops of ferromagnetic materials. If we do not know material constants, but we know the shape of hysteresis loop of material, we can use model, which uses controlled resource for simulation of material's hysteresis loop.

## 5 SENSOR SIMULATION MODEL

Sensor model was created by passive elements and by non-linear current and voltage sources. Model is separated into four basic blocks, as shown on Fig. 4.

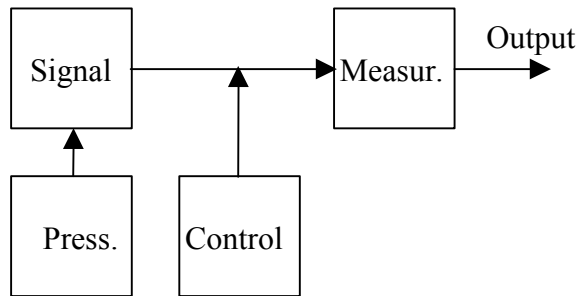


Fig. 4: Basic block scheme

### 5.1 Block „signal“

In block „signal“ the entry signal is processed in dependence from the basic parameters and magnetic features of sensor. It comes to the signal deformation, which is done by the hysteresis loop of the sensor. Current of controlled voltage source simulates the hysteresis loop. The hysteresis voltage dependency itself is simulated by polynomial of n-degree. Block „signal“ consists a source of excitation signal, entry circuit impedance, non-linear current controlled voltage source on hysteresis simulation, switching circuit, summer, limiter and block of output impedance.

### 5.2 Block „Pressure“

Block „pressure“ simulates by controlled voltage sources the mechanic pressure, which performs on the real sensor. Here can be set the constant pressure, pressure changing on time, or pressure changing on shape or direction of increase or decrease of the signal itself. Setup of the pressure depends on operation conditions of real sensor.

### 5.3 Block „Conducting“

Block „Conducting“ switches increasing or decreasing half-wave of the signal in output. It is composed from passive elements and operative amplifier. Block „Conducting“ consists of the signal detection, comparing circuit and signal limiter.

### 5.4 Block „Measuring“

In the block „Measuring“ the outputs changing signal is measured. Evaluated is effective or middle value. This block is not a sensor model, it is just a final measurement of output signal from sensor model. In our case, the effective value is evaluated, due to deformation of output signal.

### 5.5 Controlled sources

The controlled sources are one of the most useful features of PSPICE. Controlled sources measure voltage or current and use the measured value to control their output. The transformation allowed between input and output is a multidimensional polynomial. The dimension and the coefficients of the polynomial are specified. The input to be measured must be described. Single-dimension polynomial functions, which are basically the additive combination of many linear functions, are easily described using the syntax:

$$(X) \langle \text{node} \rangle \langle \text{node} \rangle \text{POLY}(1) \langle \text{inputs} \rangle \langle \text{coefficients} \rangle$$

Where X can be replaced by:

- E – voltage-controlled voltage source
- F – current-controlled current source
- G – voltage-controlled current source
- H – current-controlled voltage source

### 5.6 Complex model scheme

A complex model scheme is shown on Fig. 5. Exciting entry signal from source VIN is come on entry source HR1 and also on entry source HR2. Voltage source VMR1 is set for constant value 0V and in the circuit is represents an ampere-meter. Circuit for controlled signal is also connected on source VIN. In the bottom part of the scheme, the circuit for controlled signal is shown, which output manages switches SW31 and SW32. Hysteresis loop is simulated in parts. It is simulated separately the top part of the loop where the exciting signal is decreasing and the bottom part where the exciting signal is increasing. Top part of the scheme consists sources HR1, MULT1 a MAT1 simulates top part of the schema and the part of the scheme consisting sources HR2, MULT2 a MAT2 simulates bottom part of hysteresis loop. Block HR1 is no-linear dependent, current controlled voltage source. His function is described by polynomial of n-degree:

$$U = k_0 + I.k_1 + I^2.k_2 + I^3.k_3 + \dots \quad (6)$$

where:  $U$  is output voltage of non - linear source,  $k_n$  are coefficients of polynomial,  $I$  is controlled current merged by ampere-meter VMR1. Affecting pressure the steepness of hysteresis loop is changed, as shown on Fig. 6.

Dependency of the pressure is modelled in voltage source MULT1, where multiplying source of pressure and modelling of hysteresis loop realize the operation. Source MAT1 is used for adaptation the simulated signal in the part of hysteresis loop, which is

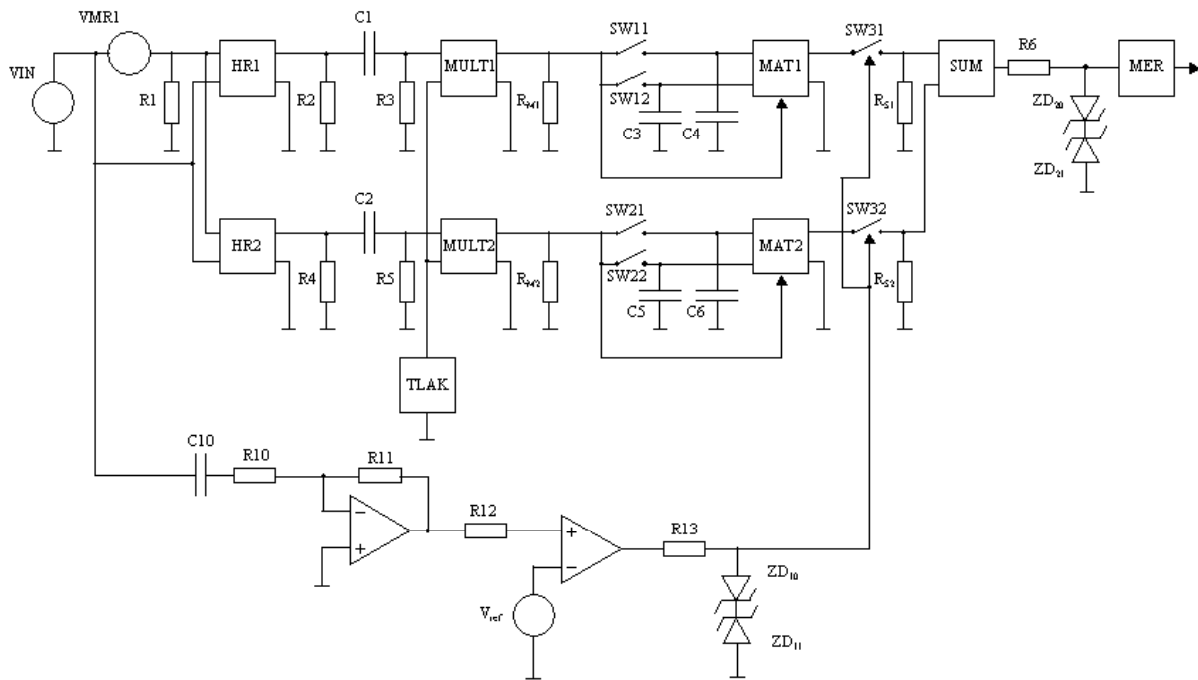


Fig. 5: Model scheme in SPICE

added from signal from source MAT2 in voltage source SUM. For correct switching of both signals there are switchers SW31 and SW32, which are switching on increased or decreased signal. Zener diodes on increase from source SUM realize the saturation state as shown on Fig. 7. The block „measuring“ is not the part of sensor simulation model, but is necessary for effective value, which is calculated as:

$$U_{ef} = \sqrt{\frac{1}{T} \int u^2(t) dt} \quad (7)$$

where:  $U_{ef}$  is effective value of output signal,  $T$  is period of the signal,  $u(t)$  is measured material.

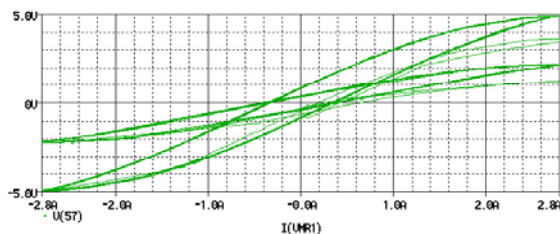


Fig. 6: Dependency of pressure

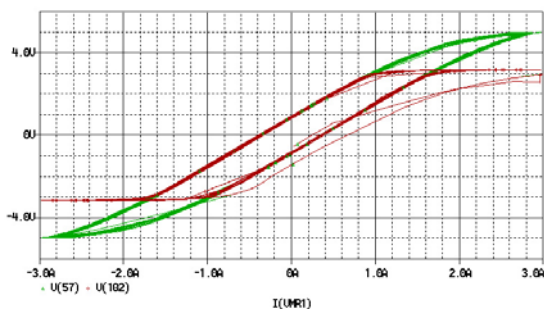


Fig. 7: Simulation state of saturation

Modes allow simulate also a reversible magnetization as it is shown on Fig. 8.

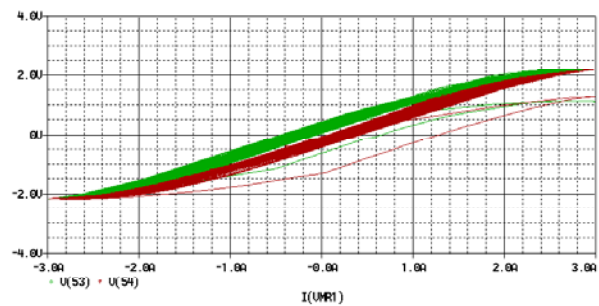


Fig. 8: Reversible magnetization

End points in first contact copy a loop of primary magnetization.

## 6 TORQUE SENSOR

Torque sensor is composed from one exciting ferromagnetic core (P), two sensing ferromagnetic cores (S) and a ferromagnetic pipe @. Primary coil consists all together 2000 coils and secondary coil 6000 coils . The sensor is shown on Fig. 9.

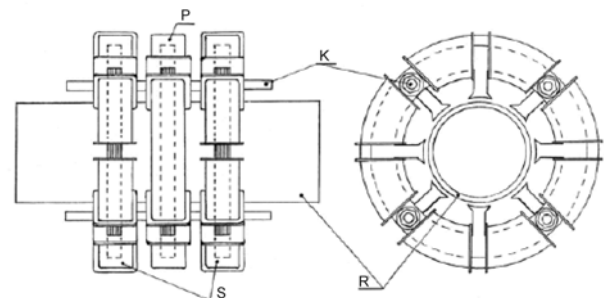


Fig. 9: Torque sensor

After charging a pipe by torque, a magnetic field is deformed. Between poles of coil there begins the magnetic voltage. Consequently, the changing magnetic flow flows by sensing core, which in the spools of sensing coil creates changing electric voltage. Change of voltage is direct on the change of the size of the torque. Simulated hysteresis loop is shown on Fig. 10.

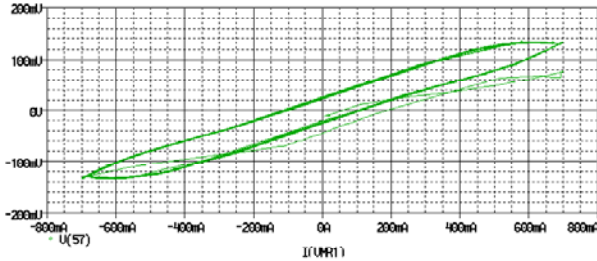


Fig. 10: Hysteresis loop of sensor

Affecting the torque, the steepness of hysteresis loop is changed as is shown on Fig. 11.

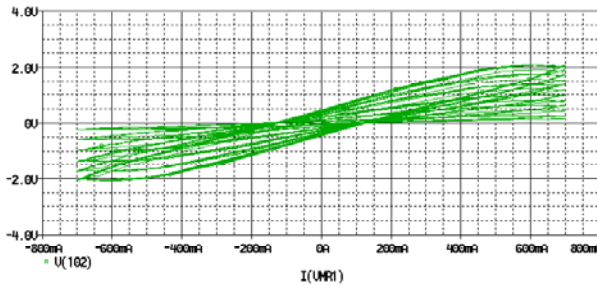


Fig. 11: Effect of torque

The error of the sensor model in comparison with real sensor is  $-0.32\%$  and  $+0.54\%$ . No-linearity is  $1.05\%$  and error of hysteresis is  $0.78\%$ . By formula (8) we can define the losses of material, when simulated hysteresis loops of several materials by polynomial n-degree.

$$z = \frac{\int_0^{H_{f \max} + H_{fC}} f_h(x) dx - \int_0^{H_{f \max} - H_{fC}} f_d(x) dx}{\int_0^{H_{g \max} + H_{gC}} g_h(x) dx - \int_0^{H_{g \max} - H_{gC}} g_d(x) dx} \cdot 100\% \quad (8)$$

This is one of the options of how to define suitable material for the elastomagnetic sensor of transformer type.

## 7 CONCLUSION

Model is build on the knowledge of the hysteresis loop used magnetic material, size of the value of excitation current and dimension of measured pressure, by which it is categorized as models which for the simulation of real sensors need minimum of entry information and eliminate one of the core problems of models of transformer types of sensors.

## 8 ACKNOWLEDGEMENT

The paper has been prepared under support of Slovak grant projects VEGA No. 1/4174/07, VEGA No. 1/0660/08, KEGA No. 3/5227/07, KEGA No. 3/6388/08 and KEGA No. 3/6386/08.

## 9 REFERENCES

- [1] Lee, E., W.: Magnetostriction and magnetomechanical effects, Department of Physics, The university Nottingham.
- [2] Tomčíková, I., Molnár, J., Vince, T.: Interakcia magnetického poľa a napätosti pre elastomagnetický snímač tlakovej sily, Elektrotechnika. No. 34, 2008, pp. 1-11.
- [3] Potocký, L., Hajko, V., Zentko, A.: Magnetizačné procesy, ALFA, Košice, 1982.
- [4] Kováč, D., Kováčová, I., Šimko, V.: Electrical Engineering II, Part Theoretical Electrical Engineering, Elfa s.r.o. Publisher, 144 pages, 2006.
- [5] Gallová, Š.: Fuzzy ontology and information access on the web, International Journal of Computer Science. Vol. 34, No. 2, 2007, pp. 234-238.
- [6] Moses, A. J.: Problems in modelling the magnetizing process for theoretical and experimental studies, Proceeding on the first Japanese – Czechoslovak joint seminar on applied electromagnetics in materials, 1992, Piešťany, Slovakia.
- [7] Bartoš, S., Doležel, I., Nečesaný, J., Škramlík, J., Valouch, V.: Theoretical and Experimental Investigation of Parasitic Effects in Induction Motor Drives Supplied from Semiconductor Inverters, Acta Electrotechnica et Informatica, Vol. 8, No. 4, 2008, s. 3-9.
- [8] Vince, T., Molnár, J., Tomčíková, I.: Remote DC Motor Speed Regulation via Internet, 10<sup>th</sup> International PhD Workshop OWD 2008, Warszawa, pp. 293-296, 2008.
- [9] <http://www.ecircuitcenter.com/index.htm>
- [10] Špánik, P., Čuntala, J., Lakatoš, J., Kondelová, A., Frivaldský, M.: Analysis of Field of Temperature of Power Electronic Systems in Comsol Multiphysics Enviroment, Electroscop, Plzeň, 2008.
- [11] Tomčíková, I.: Selected chapters from Electrical Engineering I, Košice, Elfa, 148 pages, 2005, ISBN 80-8086-017-3.
- [12] Mayer, D., Ulrych, B., Škopek, M.: Electromagnetic Field Analysis by Modern Software Products, Journal of Electrical Engineering, Vol. 7, No.1, 2001.

Dobroslav Kováč, Prof., Ing., CSc., Katedra teoretickej elektrotechniky a elektrického merania, Fakulta elektrotechniky a informatiky, Technická univerzita v Košiciach, Park Komenského 3, 042 00 Košice, E-mail: dobroslav.kovac@tuke.sk  
 Ing. Milan Peťko, RWE IT Slovakia, s.r.o., Južná trieda 6, 040 01 Košice, milan.petko@rwe.com  
 Irena Kováčová, Prof., Ing., CSc., Katedra elektrotechniky, mechatroniky a priemyselného inžinierstva, Fakulta elektrotechniky a informatiky, Technická univerzita v Košiciach, Letná 9, 042 00 Košice, E-mail: irena.kovacova@tuke.sk  
 Vojtech Šimko, Doc., Ing., CSc., KTEEM, FEI, TU v Košiciach, E-mail: vojtech.simko@tuke.sk